The paraelectric-incommensurate phase transition and crystal structure of the mixed crystals $K_x(NH_4)_{2-x}SeO_4$

1998 J. Phys.: Condens. Matter 10 5245

(http://iopscience.iop.org/0953-8984/10/24/003)

J. Phys.: Condens. Matter **10** (1998) 5245–5253. Printed in the UK PII: S0953-8984(98)90293-4

The paraelectric–incommensurate phase transition and crystal structure of the mixed crystals $K_x(NH_4)_{2-x}SeO_4$

Xavier Solans†, Catalina Ruiz-Pérez‡, Cristina González-Silgo‡, Lourdes Mestres§, M Luisa Martínez-Sarrión§ and Eduardo Bocanegra‖

† Departamento Cristallografia Mineralogia i Dipòsits Minerals, Universitat de Barcelona, Spain
‡ Departamento Física Fundamental y Experimental, Universidad de la Laguna, Spain
§ Departamento Química Inorgànica, Universitat de Barcelona, Spain
‖ Departamento Física Aplicada II, Universidad del Pais Vasco, Spain

Received 5 January 1998, in final form 20 March 1998

Abstract. A study on the mixed crystals of general formula $K_x(NH_4)_{2-x}SeO_4$ has been carried out, using thermal analyses and x-ray diffraction on powder and single-crystal samples at different temperatures. The replacement of the potassium ion by the ammonium ion is only possible for $x \geqslant 1.45$. The transitions paraelectric–incommensurate–ferroelectric are only observed for $x \geqslant 1.76$ and the temperature of the paraelectric–incommensurate transition increases when the value of x decreases. The replacement of the K^+ ion by the ammonium ion is only produced in the K(1) site. The different behaviour of the mixed crystals and the K_2SeO_4 compound is explained from the structural results.

1. Introduction

Potassium selenate has been extensively studied, since Aiki and Hukuda [1] found that it undergoes two successive transformations at $T_i = 129.5$ K (paraelectric–incommensurate transition) and $T_C = 93$ K (incommensurate–ferroelectric transition). The crystal structure of the paraelectric phase at 298 K shows the space group $Pnam$ and it is isostructural with $\beta - K_2SO_4$ [2]. Below T_i the phase is incommensurate with wave vector $\boldsymbol{q} = (1 - \delta)\boldsymbol{a}/3$, and a close correspondence was observed between the phonon instability in the paraelectric phase and the incommensurate structure, but the origin of this instability was not understood [3]. The crystal structure of the ferroelectric phase at 80 K was determined by Yamada *et al* [4], showing the space group $Pna2_1$ with $\boldsymbol{a}_{ferro} = 3\boldsymbol{a}_{para}$. González-Silgo *et al* [5] have followed the structural behaviour of K_2SeO_4 at different temperatures by x-ray diffraction, rigid body motion analysis and Brown theory [6]. They deduced that K(1) is the main ion that produces the different transitions and the rotation of selenate ion around the $\boldsymbol{b}$-axis together with the displacement of cations produces the new phase at T_i.

The study of mixed crystals in order to understand the mechanism of the phase transition of A_2BX_4-type compounds has been carried out by several authors. González-Silgo *et al* [7, 8] showed that the transition temperature descends in the mixed crystals $K_x(NH_4)_{2-x}SO_4$ and $Tl_x(NH_4)_{2-x}BeF_4$ when the value of x increases and that the orientation of the BX_4 ion around the $\boldsymbol{c}$-axis depends on the x-value at the same temperature. Also, they also pointed out the different role of the cation sites, according to the study of the translational and the librational tensors, in the first compound; and the map of the sum of the bond valence in both compounds. Mixed crystals with anion substitution $(NH_4)_2(SO_4)_x(SeO_4)_{1-x}$ [9]

0953-8984/98/245245+09$19.50

and $(NH_4)_2(SO_4)_x(BeF_4)_{1-x}$ [10] have also been studied. The replacement of sulphate by seleniate causes an increase in the Curie point, while the replacement by flourberyllate produces a decrease in the Curie temperature as in the previously mentioned mixed crystals.

$(NH_4)_2SeO_4$ (which belongs to the $A2/m$ space group [11]) and K_2SeO_4 are not isostructural at room temperature. Mixed crystals of general formula $K_x(NH_4)_{2-x}SeO_4$ were prepared in order to determine how as a badly fitting ion alters the mechanism of the paraelectric–incommensurate–ferroelectric phase transitions of K_2SeO_4. The study was carried out using thermal analyses, x-ray diffraction on powder and single-crystal samples at different temperatures.

2. Experiment and results

2.1. Synthesis

Mixed crystals were obtained by mixture of $(NH_4)_2SeO_4$ and K_2SeO_4 at 313 K on aqueous solution. Crystals were obtained by slow evaporation at the same temperature. In all cases, the number of phases was determined by x-ray diffraction, the degree of substitution was determined by analyses of N and H with a Carlo Erba microanalyser EA1108, and K and Se by ICP (induced condensed plasma) with a Jobin–Yvon analyser. The starting composition of the mixture and the obtained phase composition is given in table 1.

Table 1. Ratio of K_2SeO_4 and $(NH_4)_2SeO_4$ mixed in aqueous solution and obtained products.

	Starting composition		
Sample	K_2SeO_4 (mols)	$(NH_4)_2SeO_4$ (mols)	Obtained products
1	1.90	0.10	$K_{1.91}(NH_4)_{0.09}SeO_4$
2	1.75	0.25	$K_{1.81}(NH_4)_{0.19}SeO_4$
3	1.65	0.35	$K_{1.76}(NH_4)_{0.24}SeO_4$
4	1.40	0.60	$K_{1.45}(NH_4)_{0.55}SeO_4$
5	0.90	1.10	$[(NH_4), K]_2SeO_4 + (NH_4)_2SeO_4$
6	0.75	1.25	$[(NH_4), K]_2SeO_4 + (NH_4)_2SeO_4$
7	0.50	1.50	$[(NH_4), K]_2SeO_4 + (NH_4)_2SeO_4$

The lack of isostructurality between the two salts may explain the existence of solid solutions for $x \geqslant 1.45$.

2.2. Thermal analyses: DSC

Thermal analyses were carried out on a Perkin–Elmer differential scanning calorimeter DSC7. The samples were measured in the temperature range 80–293 K, with a warming rate of 10 K min^{-1} and a total scale sensitivity of 0.4 mW. The mass of sample was in the range 20–25 mg. Results are given in table 2.

2.3. X-ray powder diffraction

Powder diffraction data were collected at different temperatures with two instruments because of the disponibility. The samples with $x = 2$ and $x = 1.81$ were mounted on a Siemens D500 diffractometer with Bragg–Brentano geometry, using Cu Kα radiation and

Table 2. The paraelectric–incommensurate transition temperature for the mixed crystals $K_x(NH_4)_{2-x}SeO_4$.

x	Onset temperature (K)	Integrated area ΔH (J mol^{-1})
2	127	38.0
1.91	140	35.4
1.81	154	31.8
1.76	not observed	

a secondary monochromator. The measurements were carried out while the sample was cooled from 298 to 90 K. The cooling rate was 5 K min^{-1} and the sample was left for 5 min at the measuring temperature, in order to stabilize the equipment and the sample. The step size was 0.025°, the time of the step was 10 s and the 2θ range was 15–60°. The samples with $x = 1.91$ and 1.45 were measured with Debye–Scherrer geometry, using a 120° arch detector INEL, with the sample in a rotating capillary to diminish preferred orientation. The radiation was Cu Kα monochromatized by a plane primary monochromator. The cooling process was equal to that used in the Siemens instrument and the measuring time was defined by the value of the highest intensity.

The indexation of powder diffraction patterns was carried out using the TREOR computer program [12], and the cell parameters were refined with the CELREF computer program [13] (20–35 peaks were used in the refinement). The variation of the cell parameters versus the value of x and the temperature is shown in figure 1.

2.4. X-ray single-crystal diffraction

A prismatic crystal of $K_{1.81}(NH_4)_{0.19}SeO_4$ was selected and mounted on a Enraf–Nonius CAD4 diffractometer. Intensity data were collected at 293, 204 and 125 K in order to determine the geometric variations of the paraelectric phase versus the temperature. At 125 K the structure is in the incommensurate phase and the satellites peaks were observed using the oscillant technique. The intensity of satellite peaks is very weak at this temperature and was not measured, so the average structure was determined. Unit-cell parameters were determined from automatic centring of 25 reflections ($12 < \theta < 21°$). Intensities were collected using the ω–2θ scan technique; the scan width was calculated as $A + B\tan\theta$, where A was estimated from the mosaicity of crystal and B allows the increase of peak width due to Mo Kα1 and Mo Kα2 splitting. The intensity of three reflections was measured each two hours as intensity and orientation control; significant fluctuations were not detected. Intensities were corrected for Lorentz, polarization and absorption effects.

The structures were solved by isomorphic replacement from the values of K_2SeO_4 and refined with the SHELXL-93 computer program [14]. The function minimized was $w||F_o|^2 - |F_c|^2|^2$; the weighting scheme was $[\sigma^2(I) + (k_1P)^2 + k_2P]^{-1}$, where $P = (2F_o^2 + F_c^2)/3$. The values of k_1 and k_2 were computed in order to optimize the final R-values. Details of the structure refinement are listed in table 3. The occupancy factors for ammonium and potassium ions were refined independently for each site and ammonium substitution was not observed in the K(2) site. (The final K(1) occupancy factor was 0.809(7).) The atomic coordinates and equivalent isotropic temperature coefficient are listed in table 4.

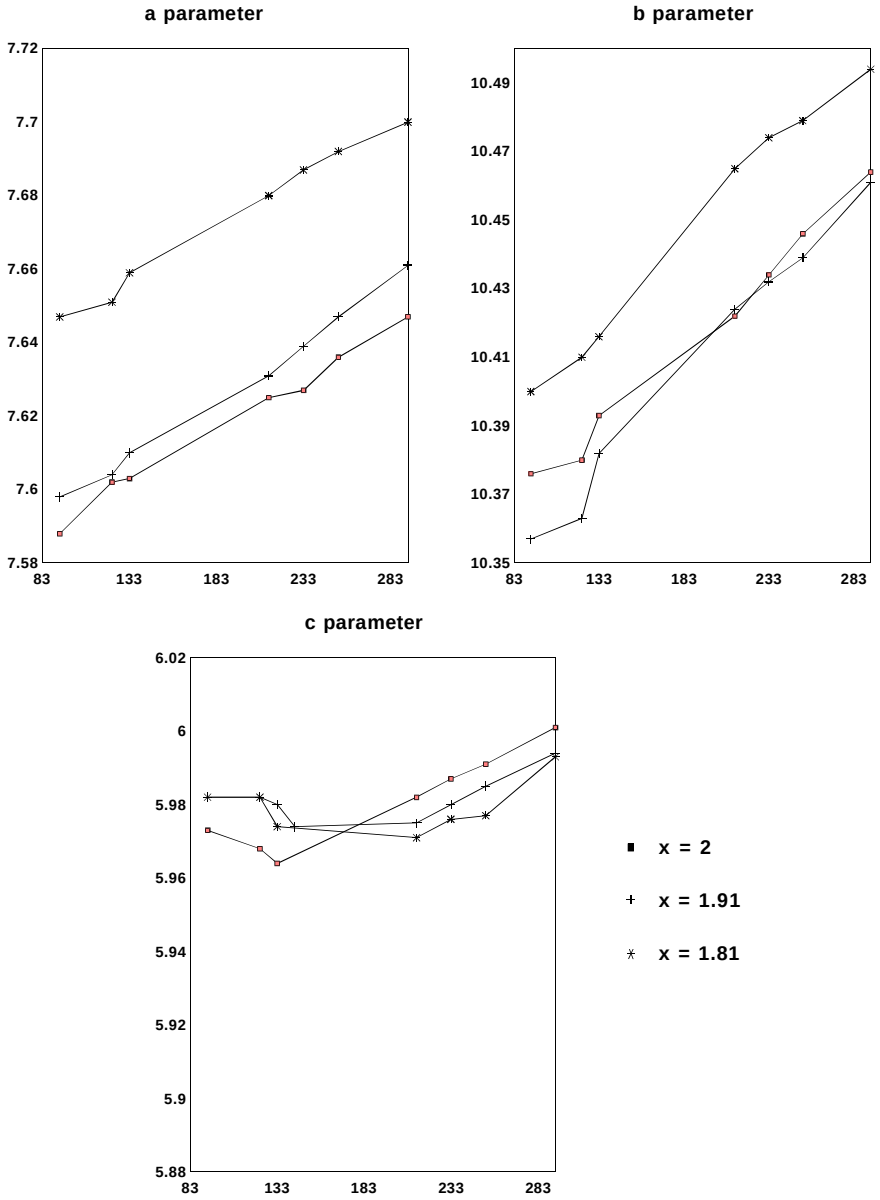

Figure 1. Variation of the cell parameters versus the temperature for different compositions of the mixed crystal $K_x(NH_4)_{2-x}SeO_4$.

3. Discussion

According to the thermal analyses, the substitution of the K^+ ion by the NH_4^+ causes an increase of the Curie temperature, decreasing the transition enthalpy. A structural study around the cation would be justified to demonstrate the role of the cation substitution

Table 3. Crystal data and structure refinement for $K_{1.81}(NH_4)_{0.19}SeO_4$.

Formula weight	216.79	216.79	216.79
Temperature (K)	293(2)	204(2)	125(2)
Wavelength (Å)	0.71069	0.71069	0.71069
Crystal system	orthorhombic	orthorhombic	orthorhombic
Space group	*Pnam*	*Pnam*	*Pnam*
a (Å)	7.6980(10)	7.6664(8)	7.6419(7)
b (Å)	10.501(5)	10.470(6)	10.422(6)
c (Å)	6.011(8)	6.001(9)	5.999(7)
Volume (Å^3)	485.9(7)	481.7(8)	477.8(6)
Z	4	4	4
Density Mg m^{-3}	2.963	2.989	3.014
μ (mm^{-1})	9.159	9.240	9.315
$F(000)$	409	409	409
Crystal size (mm^3)	$0.3 \times 0.2 \times 0.2$	$0.3 \times 0.2 \times 0.2$	$0.3 \times 0.2 \times 0.2$
θ range (°)	3.28–29.94	3.29–29.91	3.31–29.92
Index ranges	$0 \leqslant h \leqslant 10$	$0 \leqslant h \leqslant 10$	$0 \leqslant h \leqslant 10$
	$0 \leqslant k \leqslant 14$	$0 \leqslant k \leqslant 14$	$0 \leqslant k \leqslant 14$
	$0 \leqslant l \leqslant 8$	$0 \leqslant l \leqslant 8$	$0 \leqslant l \leqslant 8$
Reflexions			
collected	773	764	756
observed ($I > 2\sigma(I)$)	505	731	510
Refined parameters	43	43	43
Goodness-of-fit on F^2	1.051	1.043	0.975
R (on F) (observed)	0.065	0.068	0.071
wR (on F^2) (observed)	0.176	0.162	0.183
R (on F) (all data)	0.109	0.082	0.103
wR (on F^2) (all data)	0.330	0.195	0.263
Extinction coefficient	0.022(6)	0.054(9)	0.11(4)

in this type of phase transition. Moreover, the incommensurate phase vanished when the NH_4^+ substitution increased. A similar situation occurs for the solid solution $(NH_4)_2(BeF_4)_x(SO_4)_{1-x}$ [10].

The orthorhombic symmetry of all samples with $x > 1.45$ was confirmed by x-ray powder diffraction. At 298 K the samples with $x < 1.45$ always gave diffraction patterns corresponding to a mixture of the monoclinic $(NH_4)_2SeO_4$ with the orthorhombic phase. figure 1 shows the variation of the cell parameters versus the temperature. Parameters $\boldsymbol{a}$ and $\boldsymbol{b}$ increase their value as is replaced the K^+ by NH_4^+ ion, while the $\boldsymbol{c}$ parameter decreases with this substitution. The parameter $\boldsymbol{a}$ decreases its value as the temperature decreases, while parameters $\boldsymbol{b}$ and $\boldsymbol{c}$ have an anomalous behaviour at T_i. The x-ray powder diffraction study shows that the mixed crystals have a similar behaviour as K_2SeO_4 versus the temperature.

From the obtained data at 125 K only the main reflections were used for solving the average structure. The satellite intensities were too low for a structure determination of the incommensurate phase. It is in agreement with the study on the K_2SeO_4 incommensurate phase [4], where the modulation grows as the temperature approaches the Curie temperature and the thermal analyses study of this manuscript, where it is shown that the incommensurate phase vanished when the NH_4^+ substitution increase.

Selected interionic bond lengths and angles are listed in table 5. The Se–O bond lengths are not equivalent. The Se–O(2) length in the paraelectric phase is shorter than the remaining Se–O bond lengths, which indicates an higher electronic localization in this

Table 4. Atomic coordinates ($\times 10^4$) and equivalent isotropic displacement parameters ($\text{Å}^2 \times 10^3$) for $K_{1.81}(NH_4)_{0.19}SeO_4$. U_{eq} is defined as one-third of the trace of the orthogonalized U_{ij} tensor.

	x	y	z	U_{eq}
$T = 293$ K				
Se	2271(1)	4213(1)	2500	11(1)
O(1)	3028(9)	3511(7)	250(12)	40(2)
O(2)	2922(14)	5701(8)	2500	32(3)
O(3)	178(15)	4183(11)	2500	43(3)
K(1),N	1737(4)	867(3)	2500	22(1)
K(2)	−103(3)	7097(2)	2500	20(1)
$T = 204$ K				
Se	2267(1)	4211(1)	2500	7(1)
O(1)	3000(5)	3501(4)	257(7)	29(1)
O(2)	2983(9)	5670(5)	2500	28(2)
O(3)	162(9)	4208(7)	2500	37(2)
K(1),N	1715(2)	864(2)	2500	16(1)
K(2)	−100(2)	7090(1)	2500	13(1)
$T = 125$ K				
Se	2256(1)	4202(1)	2500	12(1)
O(1)	2975(8)	3472(6)	278(11)	33(1)
O(2)	3032(11)	5667(7)	2500	31(2)
O(3)	122(12)	4267(8)	2500	45(3)
K(1),N	1697(3)	840(2)	2500	17(1)
K(2)	−71(2)	7077(1)	2500	17(1)

bond. It alters the K–O lengths, thus the average K–O(2) length (3.197 Å) is larger than the average K–O(1) (3.031 Å) and K–O(3) (2.983 Å). This was also observed in the 'pure' compound K_2SeO_4 [5].

The substitution of K^+ by NH_4^+ is only produced in the K(1) site, according to the final refined occupancy factors, which indicates that the ions of longest radius preferentially occupy the longest hole K(1) (11-coordinated site) rather than the nine-coordinated K(2) site. According to the sum of bond valence (table 5) the K(1) site is the main cause of the phase transitions in the $K_{1.81}(NH_4)_{0.19}SeO_4$ compound, similar as occurs in K_2SeO_4 [5].

In $K_{1.81}(NH_4)_{0.19}SeO_4$, when the temperature decreases, the seleniate ion rotates clockwise around the $\boldsymbol{c}$-axis, 1.50° at 204 K and 3.45° at 125 K with respect to the position at 293 K. This fact produces the shortening of several K(1), N(1) . . . O bond lengths, in particular, of the shortest K(1), N(1) . . . O(2)(ii) (2.649(12) Å at 293 K). The stress produced by the shortening of this bond (which is nearly parallel to the $\boldsymbol{a}$-axis) causes the phase transition to the incommensurate phase with wave vector parallel to $\boldsymbol{a}$.

If we compare the $K_{1.81}(NH_4)_{0.19}SeO_4$ and the K_2SeO_4 crystal structures at room temperature the selenate ion in the non-substituted compound is turned through 3.6° clockwise around the $\boldsymbol{c}$-axis with respect to the position of this ion in the substituted compound, and the K, N . . . O bond lengths are generally greater in the replaced compound. This explains the lower sum of bond valence for the replaced compound and the higher value for T_i.

Finally, the loss of phase transition when the replacement of K^+ ion by the NH_4^+ increases can be explained using the plot of the cell-parameter ratios $\boldsymbol{a}/\boldsymbol{b}$ versus $\boldsymbol{a}/\boldsymbol{c}$ (figure 3) where the ratios for different A_2SeO_4 are shown (the values of Cs_2SeO_4 are from [15]; Rb_2SeO_4 from [16] and K_2SO_4 from [17]). The crystal structures A_2BX_4 can be

Table 5. Bond lengths (Å) for the most important K, N . . . O contacts and the sum of bond valence (u.v.) around each cation site for $K_{1.81}(NH_4)_{0.19}SeO_4$.

	293 K	204 K	125 K
K(1), N(1) . . . O(1) #0, #1	3.245(9)	3.226(5)	3.203(7)
K(1), N(1) . . . O(2) #0	3.683(10)	3.699(9)	3.769(10)
K(1), N(1) . . . O(2) #2	2.649(12)	2.644(9)	2.620(9)
K(1), N(1) . . . O(1) #4, #5	2.981(8)	2.984(7)	2.988(7)
K(1), N(1) . . . O(1) #6, #7	3.245(8)	3.219(5)	3.203(7)
K(1), N(1) . . . O(3) #6, #7	3.022(4)	3.016(5)	3.012(4)
K(1), N(1) . . . O(3) #5	3.367(11)	3.281(7)	3.211(9)
Sum of bond valence	0.863(4)	0.884(3)	0.916(3)
K(2) . . . O(3) #0	2.752(11)	2.792(7)	2.790(9)
K(2) . . . O(2) #0	3.068(12)	3.023(8)	2.932(9)
K(2) . . . O(1) #8, #9	2.736(7)	2.741(9)	2.731(6)
K(2) . . . O(3) #10	2.752(9)	2.768(5)	2.763(6)
K(2) . . . O(1) #11, #12	2.866(8)	2.840(5)	2.833(7)
K(2) . . . O(2) #11, #12	3.293(6)	3.294(5)	3.311(5)
Sum of bond valence	1.193(4)	1.198(3)	1.239(3)
Symmetry code			
#0	x, y, z	#1 $x, y, 1/2-z$	#2 $1/2+x, 1/2-y, z$
#3	$1/2+x, 1/2-y, 1/2-z$	#4 $x-1/2, 1/2-y, z$	#5 $x-1/2, 1/2-y, 1/2-z$
#6	$1/2-x, y-1/2, -z$	#7 $1/2-x, y-1/2, z+1/2$	#8 $1/2-x, 1/2+y, -z$
#9	$1/2-x, y+1/2, z+1/2$	#10 $x-1/2, 3/2-y, z$	#11 $-x, 1-y, -z$
#12	$-x, 1-y, z+1/2$		

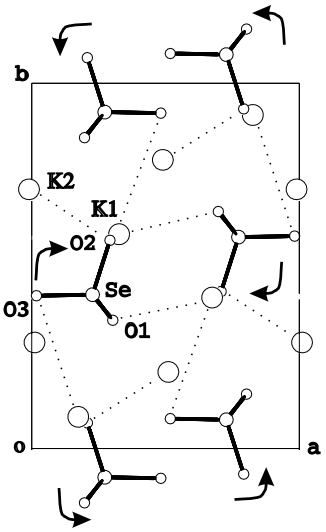

Figure 2. Unit-cell content viewed down the ***c***-axis at 293 K. Dotted line indicates the increasing contacts and the rotation of selenate ion around the ***c***-axis is also marked.

described as a distorted hexagonal packing of BX_4 anions, where the A cations occupy the octahedral hole. The $\boldsymbol{a}/\boldsymbol{c}$-ratio indicates the compactness of the structure; for the compact hexagonal packing this ratio is equal to 1.633, while the $\boldsymbol{a}/\boldsymbol{b}$-ratio indicates the asymmetry

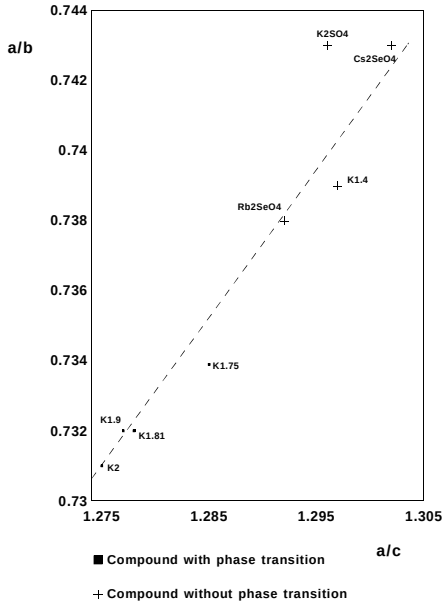

Figure 3. Plot of the lattice parameter ratios a/b versus a/c of selenates and mixed crystals.

of the octahedral hole (the higher values indicate a more symmetric hole). According to the Brown theory, the transitions occur if the packing is low and the asymmetry of the A ion site is high. When the replacement of K^+ ion by NH_4^+ increases, the values of cell parameters correspond to stable phases as observed by thermal analysis (figure 3).

Acknowledgment

This work was sponsored by financial support from CICYT (MAT95-0218 and MAT97-0371).

References

[1] Aiki K and Hukuda K 1969 *J. Phys. Soc. Japan* **26** 1066
[2] Kàlman A K, Stephens J S and Cruickshank D W J 1970 *Acta Crystallogr.* B **26** 1451
[3] Iizumi M, Axe J D and Shirane G 1977 *Phys. Rev.* B **27** 4392
[4] Yamada N, Ono Y and Ikeda T 1984 *J. Phys. Soc. Japan* **53** 2565.
[5] González-Silgo C, Solans X, Ruiz-Pérez C, Martínez-Sarrión M L, Mestres L 1996 *Ferroelectrics* **177** 191
[6] Brown I D 1992 *Acta Crystallogr.* B **48** 553
[7] González-Silgo C, Ruiz-Pérez C, Solans X, Martínez-Sarrión M L, Mestres L and Bocanegra E 1996 *J. Phys.: Condens. Matter* **9** 2657
[8] González-Silgo C, Solans X, Ruiz-Pérez C, Martínez-Sarrión M L, Mestres L and Bocanegra E in preparation

[9] Martínez-Sarrión M L, Rodríguez-Clemente A, Mestres L, Lozano A and Solans X 1991 *Ferroelectrics* **120** 271
[10] González-Silgo C, Ruiz-Pérez C, Solans X, Martínez-Sarrión M L, Mestres L, Rodríguez-Clemente A and Bocanegra E 1996 *Ferroelectrics* **175** 207
[11] Carter R L, Koerntgen C and Margulis T N 1976 *Acta Crystallogr.* C **32** 592
[12] Werner P E, Ericksson L and Westdhal M 1985 *J. Applied Crystallogr.* **18** 360
[13] Laugier J and Filhol A 1978 *CELREF* (Grenoble: Institute Langevin)
[14] Sheldrick G M 1993 *SHELXL. Program for Crystal Structure Refinement* University of Göttingen
[15] Zúñiga F, Breczewsky T and Arnaiz A 1981 *Acta Crystallogr.* C **47** 638
[16] Takahashi J, Onodera A and Shiozaki Y 1987 *Acta Crystallogr.* C **43** 179
[17] Arnold H, Kurtz W, Richter-Zinnius A and Bethke J 1981 *Acta Crystallogr.* B **37** 1643